

See discussions, stats, and author profiles for this publication at: <https://www.researchgate.net/publication/7944365>

Synthesis of Peapods Using Substrate-Grown SWNTs and DWNTs: An Enabling Step Toward Peapod Devices

ARTICLE *in* NANO LETTERS · FEBRUARY 2005

Impact Factor: 13.59 · DOI: 10.1021/nl049854y · Source: PubMed

CITATIONS

31

READS

16

4 AUTHORS, INCLUDING:



Satish B Chikkannanavar

Ford Motor Company

22 PUBLICATIONS 431 CITATIONS

SEE PROFILE



D. E. Luzzi

Northeastern University

134 PUBLICATIONS 4,740 CITATIONS

SEE PROFILE



a t charlie Johnson

University of Pennsylvania

231 PUBLICATIONS 10,129 CITATIONS

SEE PROFILE

Synthesis of Peapods Using Substrate-Grown SWNTs and DWNTs: An Enabling Step Toward Peapod Devices

Satishkumar B. Chikkannanavar[†] and David E. Luzzi^{*}

Department of Materials Science and Engineering, University of Pennsylvania, Philadelphia, Pennsylvania 19104

Scott Paulson[‡] and Alan T. Johnson, Jr.^{*}

Department of Physics and Astronomy, University of Pennsylvania, Philadelphia, Pennsylvania 19104

Received January 23, 2004; Revised Manuscript Received October 6, 2004

ABSTRACT

We report the successful synthesis of nanoscale peapods from single-walled and double-walled nanotubes grown by chemical vapor deposition (CVD) on substrates with windows etched into free-standing silicon nitride membranes. CVD-grown nanotubes were oxidized in air, then filled with C₆₀ molecules from the vapor phase. Observed variation in nanotube oxidation and C₆₀ packing with nanotube diameter agreed with theoretical expectations. Windowed samples provide several important advantages for property measurements of peapods and other nanomaterials. Individual nanostructures can be followed through processing steps, and a single nanostructure can be inspected by high-resolution TEM and subsequently contacted with nanoscale electrodes using electron beam lithography.

The novel structural, chemical, and transport properties of single-walled carbon nanotubes (SWNTs)^{1,2} have elicited tremendous interest in the scientific community. Filling of molecular materials (e.g., fullerenes,^{3–5} filled fullerenes,^{6,7} halides,⁸ and metals⁹) inside the nanotube structure provides a promising route toward producing hierarchical nanoscale materials with a wide degree of functionality. As a prototype example, it has been demonstrated that SWNTs filled with C₆₀, known as “peapods”, are a unique material, different from both the nanotube and one-dimensional (1D) chain of C₆₀ molecules. Moreover, excellent agreement was found between ultrahigh vacuum scanning tunneling microscopy (UHV–STM) data of the local density of states and the electronic structure model for peapods, where the C₆₀ molecular orbital hybridizes with the conduction band of a semiconducting nanotube.^{5,10}

Despite the great potential that tunable nanotubes would afford for devices, and the success in filling nanotubes with

a variety of materials, there is little experimental work on electrical transport of individual peapods.^{11,12} Two major obstacles prevent the facile electrical characterization of peapod samples. To date, peapods have been produced from bulk nanotube material; after filling, the material is suspended in solvent and then cast onto a substrate^{4,5} in order to fabricate electrodes for measurement. This processing frequently leads to high-resistance contacts, presumably due to impurity material that contaminates the nanotube wall. However, circuits fabricated from nanotubes grown by chemical vapor deposition (CVD) can have nearly transparent contacts with quantum limited resistances,¹³ enabling the observation of intrinsic transport phenomena such as the Kondo effect¹⁴ and Fabry–Perot interference.¹⁵ Peapods present an additional challenge to microstructure measurement, as atomic force microscopy (AFM) and scanning electron microscopy (SEM), conventionally used to characterize nanotubes, are incapable of determining whether a given nanotube is filled or not. While transmission electron microscopy (TEM) is ideal for microstructure characterization, TEM samples are usually incompatible with lithography processes, and therefore transport measurements. It is clearly desirable to develop a

^{*} Corresponding authors. E-mail: luzzi@lrs.m.upenn.edu; cjohnson@dept.physics.upenn.edu.

[†] Current address: Analytical Chemistry Sciences, Los Alamos National Laboratory, Los Alamos, NM 87545.

[‡] Current address: Department of Physics, James Madison University, Harrisonburg, VA 22807.

sample geometry that enables microstructure characterization and transport measurement of the *same* peapod sample.

In this letter we present a novel approach of filling individual CVD-grown carbon nanotubes with C_{60} molecules, wherein the sample substrates are compatible with both microstructure characterization and electrical transport measurements. Our CVD synthesis yields single-walled and double-walled nanotubes (DWNTs) of varying diameters, which we have filled successfully with C_{60} molecules. These CVD-based peapods are produced without any acid-based processing, thereby avoiding the problems observed in solution processed nanotube samples. The nanotubes are grown on free-standing silicon nitride membranes, with micrometer-sized holes machined completely through the membrane. The holes facilitate TEM imaging for microstructure characterization, while the membrane is a suitable support for further lithography and thin-film deposition. These substrates should allow us to combine TEM and transport measurement, two complementary and powerful techniques, for nanoscale material characterization.

To synthesize peapods from CVD-grown nanotubes, we start with double-sided polished (100) silicon wafers with 100 nm of low-stress silicon nitride deposited on each side. Specific regions of the silicon substrate are removed using photolithography and anisotropic etching in an aqueous KOH solution to leave suspended silicon nitride membranes roughly 100 μm on a side. Electron beam lithography followed by a SF_6 plasma etch is then used to create an array of 2- μm -diameter holes in the membrane (Figure 1A). A 50 nm layer of silicon oxide is deposited on the windowed substrate, and SWNTs and/or DWNTs are subsequently grown by chemical vapor deposition using an iron(III) nitrate solution (typically 50–150 mg in 1 L of 2-propanol) as the catalyst source.^{16,17}

Samples were characterized by TEM using a JEOL 2010F and a JEOL 2010 operating at 100 kV and 80 kV, respectively, and a specially designed specimen cartridge. Typically 50–60% of the windows are crossed by nanotube structures, and this fraction increased at higher catalyst concentrations. SWNTs, SWNT bundles, and DWNTs are all found in the growth product, with the latter two becoming more common as the catalyst concentration increases. One benefit of this substrate geometry is apparent from Figure 1C–E. Since these structures have approximately equal diameter, they cannot be distinguished by AFM or SEM. However, their different microstructure is readily apparent in TEM. Information on amorphous carbon coverage can also be obtained for better understanding of the CVD growth process. SWNT diameters are in the range of 1–5 nm. DWNTs grown by CVD have inner and outer diameters of 0.7–4.7 nm and 1.4–5.5 nm respectively, with a van der Waals separation of ~ 0.35 nm between the concentric nanotube layers. Occasionally we see small bundles of 3–6 DWNTs, as found by others for bulk growth.^{18,19}

To encapsulate C_{60} within nanotubes, it is necessary to create defects in the cage that allow C_{60} access to the nanotube lumen. We explored both air oxidation and acid treatment (HCl , HNO_3 , H_2O_2) as candidate routes for opening

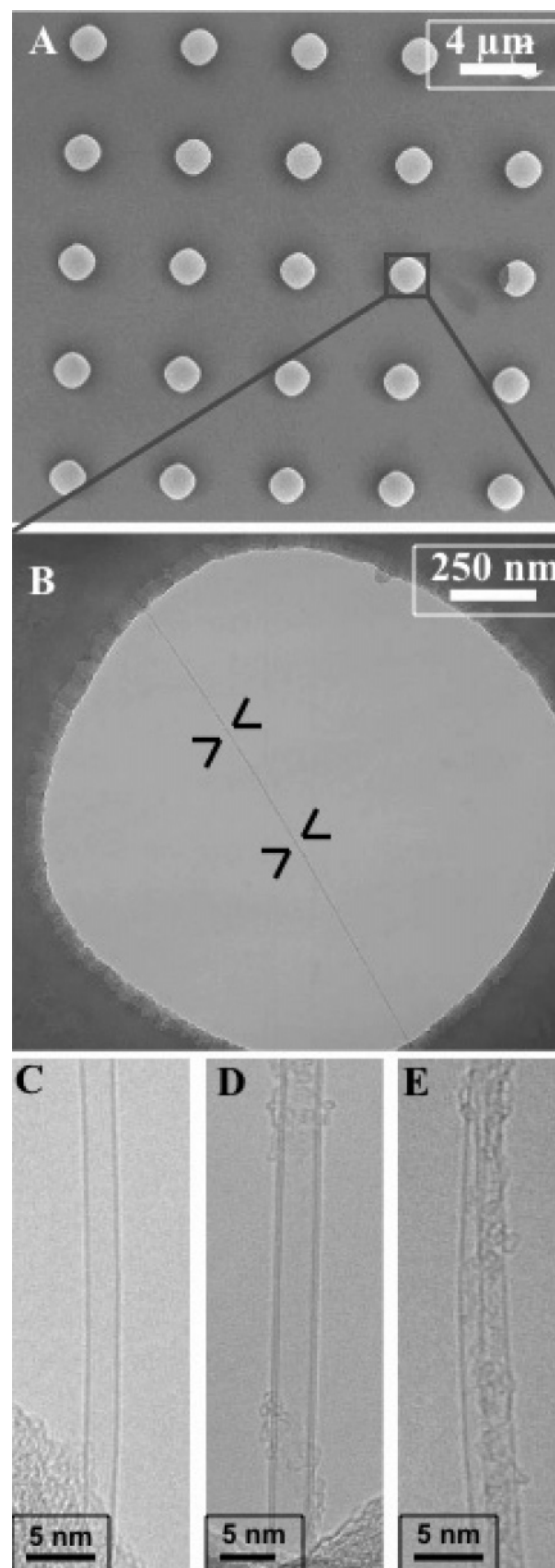


Figure 1. (A) Low magnification TEM micrograph of a SiN_4/Si substrate. The dark area is the 100-nm-thick membrane, the light circles are the lithographically defined micron-sized holes. (B) Close up of a single hole, featuring an individual SWNT suspended across it. (C–E) show, respectively, HRTEM images of a SWNT, DWNT, and a SWNT rope grown during the CVD process.

of the nanotubes grown on windowed substrates and had far greater success with the former approach. From work on bulk nanotube material, it is known that air oxidation at temper-

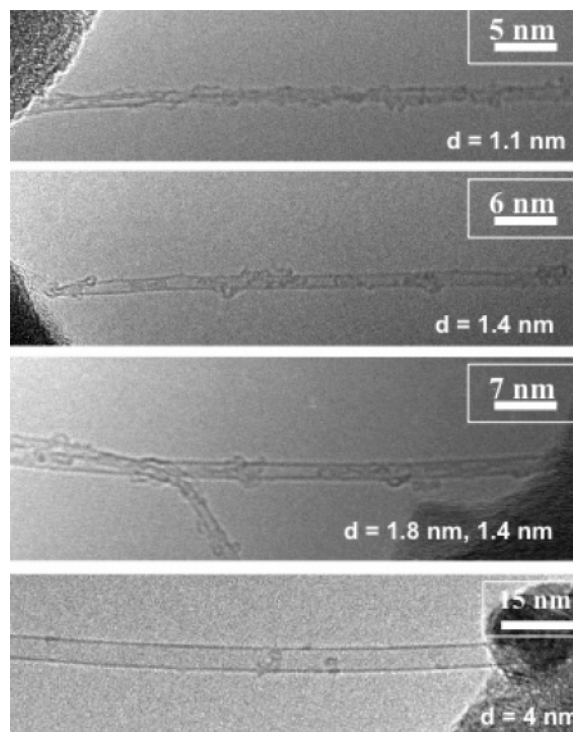


Figure 2. TEM micrographs illustrating the effect of air oxidation (300 °C for 6 h) on SWNTs with various diameters. (A) SWNT of ~1 nm diameter shows disruption along the nanotube cylindrical structure; (B) and (C) SWNTs showing a moderate change due to air oxidation; and (D) SWNT of large diameter with no apparent structure disruption due to lower strain and hence higher resistance to air oxidation.

atures near 350 °C is an effective method to purify and open the nanotubes.⁹ In the present work, air oxidation at 300 °C for 6 h produced best results in the later filling experiments.

We studied the effect of air oxidation at 300 °C for 6 h on individual nanotubes that were visible in TEM on windowed substrates. We observed that the degree of damage experienced by tubes due to oxidation decreases with increasing nanotube diameter, as illustrated in Figure 2A–D. The graphitic network is seriously disrupted after oxidation for nanotubes with diameter ~1 nm (Figure 2A), while nanotubes of 4 nm diameter (Figure 2D) remain largely intact. Oxidation leads to marginal structure modifications in intermediate diameter SWNTs (Figure 2B,C). This result agrees with the finding of preferential combustion of small diameter nanotubes in bulk material.²⁰ It provides direct evidence for the important role of nanotube diameter in determining chemical reactivity, as expected since carbon–carbon bonds are more strained in smaller diameter nanotubes,²¹ and therefore more readily oxidized. Although no effect of oxidation is visible in Figure 2D, nanotubes of this large diameter are presumably damaged by the process, most likely at the ends, since they are readily filled with C₆₀ by the process described in the next paragraph. One advantage of the windowed substrate is that individual nanotubes can be followed through processing steps. As an example, the *same* nanotube is shown before and after oxidation in Figure 3 A,B. Although the only visible effect on the nanotube is a slight reduction in amorphous carbon coating, the coated

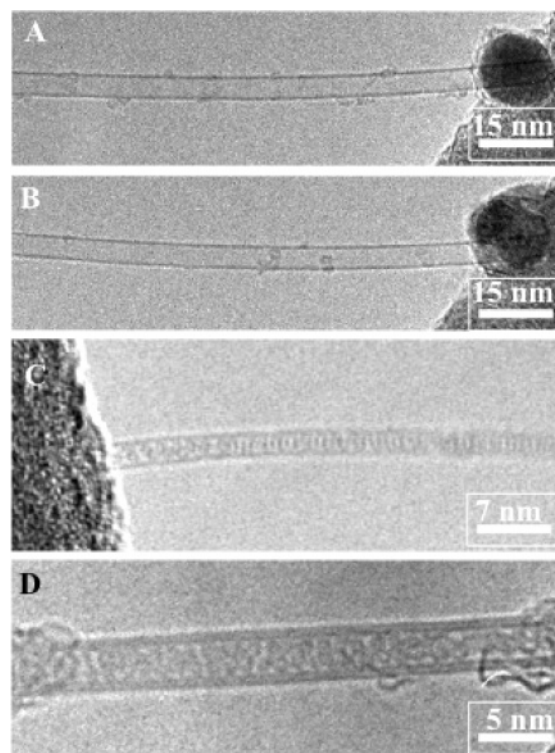


Figure 3. TEM images tracking a SWNT undergoing air oxidation prior to filling: (A) the starting nanotube, (B) the same nanotube after air oxidation at 300 °C for 6 h, (C and D) micrographs of a SWNT and DWNT filled with C₆₀ molecules using the protocol described in the text.

metal catalyst particle adjacent to the nanotube shows a strong contrast change due to oxidation.

For the purpose of filling after air oxidation, samples were inserted in a quartz ampule along with C₆₀ powder (resublimed to achieve purity >99.9%). The ampule was evacuated to below 10^{−6} Torr and held at 350 °C for 2–4 h under vacuum; the ampule was then sealed. The ampule was then heated to 500–550 °C, above the sublimation temperature of C₆₀, and held at this temperature for 18–24 h to carry out filling.

Successful examples of nanotube filling following air oxidation are illustrated in Figure 3C,D, which show that both SWNTs and DWNTs are readily filled. The fact that DWNTs fill easily suggests that oxidative damage occurs at the same region in the two concentric shells, likely because once the larger diameter outer shell is penetrated, oxidation damage occurs quickly in exposed regions of the more strained inner shell. The question of whether filling occurs through open ends of nanotubes or at sidewall defects along the nanotube length remains unanswered after this investigation and will be the focus of further experiments.

Encapsulated C₆₀ molecules experience a van der Waals interaction with each other and with the nanotube sidewalls. C₆₀ molecules confined in a nanotube with diameter near 1.4 nm (the sum of the C₆₀ diameter and twice the planar separation of graphite) are expected to form an ordered linear chain, while larger nanotube diameters allow more complex arrangements,^{22,23} such as a staggered chain (Figure 3C; SWNT diameter 2.1 nm) and a disordered C₆₀ nanosolid

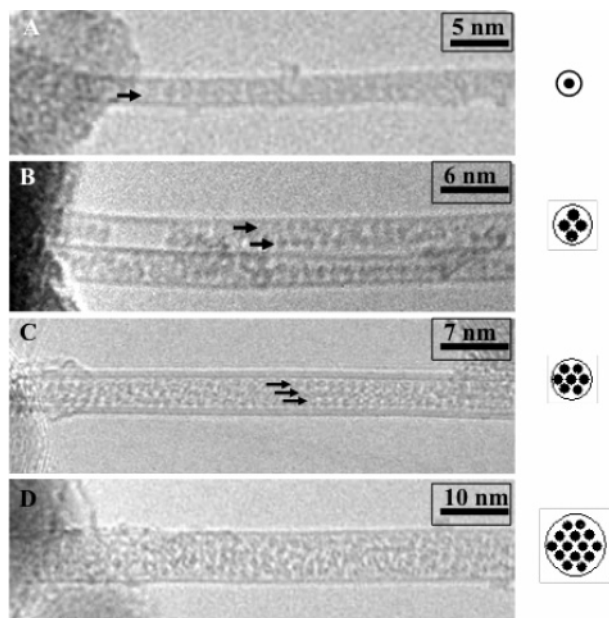


Figure 4. HRTEM images of SWNT and DWNT samples filled with fullerene molecules in various structural phases. (A) SWNT of diameter ~ 1.8 nm filled with a linear chain of C_{60} molecules, (B) SWNT (diameter ~ 3 nm) filled (on the top) with two linear chains of C_{60} molecules which show triangular crystalline lattice (see arrows), (C) DWNT (diameter ~ 3.5 nm) filled with ordered multilayers of C_{60} , and (D) SWNT of diameter 6.5 nm filled with C_{60} molecules which form a random network.

(Figure 3D; DWNT inner diameter 3.4 nm). The wide range of nanotube diameters typical of CVD growth lets this phenomenon be explored more fully as seen in Figure 4. We observe a transition from linear to multilayered stacking of the encapsulated C_{60} molecules as the inner diameter of the encapsulating nanotube increases.

Finally we demonstrate that these windowed substrates are compatible with lithographic processing. Nanotubes were located on a windowed substrate by TEM, and Cr/Au source and drain electrodes were patterned in desired locations using electron beam lithography (JEOL 6400 SEM with a Raith Elphy-Plus controller) and thin-film deposition so as to contact a nanotube network. Figure 5A shows the large scale view of the circuit formed in this manner, while in Figure 5B we see that contacting was largely successful, although there was a slight misalignment (~ 200 nm) of the electrode pattern. Electrical transport measurements on samples of this type are in progress.

To summarize, we have successfully synthesized nanoscopic peapods from SWNTs and DWNTs grown by CVD on substrates with windows fabricated in free-standing silicon nitride membranes. The process entails CVD growth of SWNTs and DWNTs on substrates, followed by controlled oxidation and filling with C_{60} molecules from the vapor phase. We found that oxidative damage is more pronounced in smaller diameter nanotubes, as expected due to their higher curvature, and we observed transitions in the C_{60} packing geometry with increasing nanotube diameter. The windowed substrate geometry offers distinct advantages for property measurement of nanomaterials: individual nanostructures can

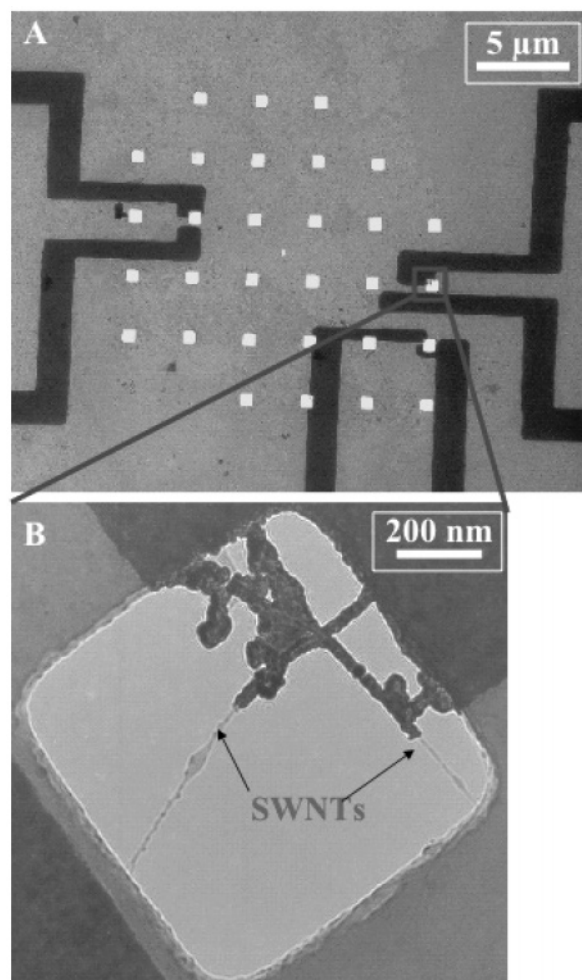


Figure 5. TEM micrographs of SWNTs contacted with gold electrodes for electrical transport measurements. Panel (A) shows how multiple nanotube samples can be contacted and (B) shows a crossed junction of SWNTs contacted with electrodes.

be followed through a series of processing steps, and the *same* nanostructure can be inspected by high-resolution TEM and contacted by nanoscale electrodes formed by electron beam lithography. We expect this will provide a powerful experimental tool for controlled investigations of nanotube peapods and other intriguing nanomaterials.

Acknowledgment. B.C.S. and D.E.L. acknowledge support from the U.S. Office of Naval Research through grant N00014-00-1-0482. Authors S.P. and A.T.J. acknowledge financial support through the Nanotechnology Institute of the Commonwealth of Pennsylvania and the University of Pennsylvania MRSEC program through grant DMR00-79909.

References

- (1) *Carbon Nanotubes: Synthesis, Structure, Properties and Applications*; Dresselhaus, M. S., Dresselhaus, G., Avouris, Ph., Eds.; Springer: New York, 2001.
- (2) Rao, C. N. R.; Satishkumar, B. C.; Govindaraj, A.; Nath, M. *ChemPhysChem* **2001**, 2, 78–105.
- (3) Smith, B. W.; Monthieux, M.; Luzzi, D. E. *Nature* **1998**, 396, 323–324.

- (4) Smith, B. W.; Russo, R. M.; Chikkannanavar, S. B.; Luzzi, D. E. *J. Appl. Phys.* **2002**, *91*, 9333–9340.
- (5) Hornbaker, D. J.; Kahng, S.-J.; Misra, S.; Smith, B. W.; Johnson, A. T.; Mele, E. J.; Luzzi, D. E.; Yazdani, A. *Science* **2002**, *295*, 828–831.
- (6) Smith, B. W.; Achiba, Y.; Luzzi, D. E. *Chem. Phys. Lett.* **2000**, *331*, 137–142.
- (7) Hirahara, K.; Suenaga, K.; Bandow, S.; Kato, H.; Okazaki, T.; Shinohara, H.; Iijima, S. *Phys. Rev. Lett.* **2000**, *85*, 5284–5287.
- (8) Sloan, J.; Kirkland, A. I.; Hutchison, J. L.; Green, M. L. H. *Chem. Commun.* **2002**, 1319–1332.
- (9) Chikkannanavar, S. B.; Taubert, A.; Luzzi, D. E. *J. Nanosci. Nanotech.* **2003**, *3*, 159–163.
- (10) Kane, C. L.; Mele, E. J.; Johnson, A. T.; Luzzi, D. E.; Smith, B. W.; Hornbaker, D. J.; Yazdani, A. *Phys. Rev. B* **2002**, *66*, 235423-1.
- (11) Chiu, P. W.; Gu, G.; Kim, G. T.; Philipp, G.; Roth, S.; Yang, S. F.; Yang, S. *Appl. Phys. Lett.* **2001**, *79*, 3845.
- (12) Shimada, T.; Ohno, Y.; Okazaki, T.; Sugai, T.; Suenaga, K.; Kishimoto, S.; Mizutani, T.; Inoue, T.; Taniguchi, R.; Fukui, N.; Okubo, H.; Shinohara, H. *Physica E* **2004**, *21*, 1089.
- (13) Soh, H. T.; Quate, C. F.; Morpurgo, A. F.; Marcus, C. M.; Kong, J.; Dai, H. *Appl. Phys. Lett.* **1999**, *75*, 627–629.
- (14) Nygard, J.; Cobden, D. H.; Lindelof, P. E. *Nature* **2000**, *408*, 342–346.
- (15) Liang, W.; Bockrath, M.; Bozovic, D.; Hafner, J.; Tinkham, M.; Park, H. *Nature* **2001**, *411*, 665–669.
- (16) Freitag, M.; Radosavljevic, M.; Zhou, Y. X.; Johnson, A. T. *Appl. Phys. Lett.* **2001**, *79*, 3326.
- (17) Hafner, J. H.; Cheung, C. L.; Oosterkamp, T. H.; Lieber, C. M. *J. Phys. Chem. B* **2001**, *105*, 743.
- (18) Ren, W.; Li, F.; Chen, J.; Bai, S.; Cheng, H.-M. *Chem. Phys. Lett.* **2002**, *359*, 196–202.
- (19) Zhu, J.; Yudasaka, M.; Iijima, S. *Chem. Phys. Lett.* **2002**, *380*, 496–502.
- (20) Zhou, W.; Ooi, Y. H.; Russo, R.; Papanek, P.; Luzzi, D. E.; Fischer, J. E.; Bronikowski, M. J.; Willis, P. A.; Smalley, R. A. *Chem. Phys. Lett.* **2001**, *350*, 6–14.
- (21) Hernandez, E.; Goze, C.; Bernier, P.; Rubio, A. *Phys. Rev. Lett.* **1998**, *80*, 4502–4505.
- (22) Hodak, M.; Girifalco, L. A. *Phys. Rev. B* **2003**, *67*, 075419-1–075419-4.
- (23) Mickelson, W.; Aloni, S.; Han, W. Q.; Cumings, J.; Zettl, A. *Science* **2003**, *300*, 467–469.

NL049854Y